Journal of the Korean Ceramic Society
Vol. 45, No. 12, pp. 766~771, 2008.

An SOFC Cathode Composed of $LaNi_{0.6}Fe_{0.4}O_3$ and $Ce(Ln)O_2$ (Ln=Sm, Gd, Pr)

Reiichi Chiba†, Takeshi Komatsu, Himeko Orui, Hiroaki Taguchi, Kazuhiko Nozawa, and Hajime Arai

NTT Energy and Environment Systems Laboratories 3-1, Morinosato-Wakamiya, Atsugi-shi, Kanagawa, 243-0198, Japan
(Received October 14, 2008; Revised December 17, 2008; Accepted December 22, 2008)

ABSTRACT

We fabricated single cells with a cathode consisting of a $LaNi_{0.6}Fe_{0.4}O_3$-$Ce_{0.8}Sm_{0.2}O_{1.9}$ composite (LNF-S20DC composite) active layer and an LNF current collecting layer on a $0.89ZrO_2$-$0.10Sc_2O_3$-$0.01Al_2O_3$ electrolyte sheet. The cathode layers were prepared by the screen-printing method. The cathode properties of these cells were measured by the AC impedance method at 800°C. The cathodes with the ceria-LNF composite active layer exhibited high power performance prior to current loading. We investigated the influence of the mixture ratio of LNF and S20DC on the cathodes properties. The Sm in the ceria particles of the composite cathode was substituted with other rare-earth elements. Cathodes with Pr and Gd co-doped ceria in the active layer provided the better performance than those with Sm- or Gd-doped ceria.

***Key words*: SOFC, Electrochemistry, Cerium compounds, Cathode, Impedance, LNF, Pr**

1. Introduction

Solid oxide fuel cells (SOFCs) are expected to enable efficient power generating systems to be realized that offer flexibility as regards system scale and fuel selection.[1,2] Medium scale SOFC systems (several kW to 100 kW systems) operating at intermediate temperatures are suitable for power generation in office buildings including telecommunications central offices or data centers.

We have been investigating $0.89ZrO_2$-$0.10Sc_2O_3$-$0.01Al_2O_3$ as an electrolyte for SOFCs operating at intermediate temperatures, because it has high oxide ion conductivity.[3]

We have also been investigating $LaNi_{0.6}Fe_{0.4}O_3$ (LNF) as a cathode material for use at intermediate temperatures,[4] because it has certain advantages including high electrical conductivity, a desirable thermal expansion coefficient,[5] high cathode performance[5-9] and high durability against chromium poisoning.[10-12]

LNF poses certain problems that must be overcome. $La_2Zr_2O_7$ tends to be formed at the interface with a zirconia electrolyte in a high temperature sintering process.[7,13] As a result the initial performance of a LNF cathode is insufficient although it gradually improves with cell operation time.[7,13-15] This limits the sintering temperature to around 1000°C. Moreover, the sinterability of LNF is low and its adhesiveness is insufficient at such a low sintering temperature.[16]

To solve these problems, we introduced an LNF-ceria composite active layer.[16] When the LNF particles are larger than those of ceria, they become covered with ceria. This can prevent the LNF particles from coming into direct contact with the zirconia electrolyte. $Ce_{0.8}Sm_{0.2}O_{1.9}$ (S20DC) is known to be a good oxide ion conductor, and the interface between the doped ceria and perovskite oxides is very stable. If LNF is used with ceria as a composite cathode, $La_2Zr_2O_7$ formation can be prevented.[13,16-18] Then the sintering temperature can be increased, and the initial cathode performance can be improved.[13,16] Increasing the sintering temperature improves the adhesiveness of the interface. In the composite active layer, there are many ceria and LNF contact points that are potentially triple phase boundaries (TPB). So we expect the TPB to be increased with this composite microstructure.

In this study, we focused on the influence of the active layer composition, sintering temperature and lanthanide element doped in the CeO_2 on the cathode properties. The properties of a cathode with an active layer, which is a mixture of ionic and electronic conductors, may be greatly influenced by their mixing ratio. This can be described in terms of the percolation theory as a Ni-YSZ anode.[1] We investigated Sm, Gd and Pr as dopants for the CeO_2 in the LNF-ceria composite active layer. Sm and Gd are typical dopants for use in increasing the oxide ion conductivity.[1] It is known that doping a small amount of Pr provides hole conduction in CeO_2.[19] A p-type conductor can exhibit high conductivity in a cathode atmosphere (high oxygen partial pressure condition). And oxide ion conduction and p-type conduction can be compatible in such an atmosphere. Therefore Pr doped CeO_2 can be an ideal mixed conductor for use in an SOFC cathode.

†Corresponding author : Reiichi Chiba
E-mail : chiba@aecl.ntt.co.jp
Tel : +82-46-240-3755 Fax : +82-46-270-2702

2. Experiments

2.1. Cell preparation

We fabricated single cells that have a cathode (consisting of an active layer and an LNF current correction layer), a Pt anode and an $0.89ZrO_2$-$0.10Sc_2O_3$ -$0.01Al_2O_3$ electrolyte sheet[3] (3.5 cm in diameter, 0.02 or 0.1 cm thick). The active layer was a composite consisting of LNF and ceria. Pastes containing S20DC and LNF particles were prepared as the screen-printing inks for the active layers. The average diameters of the LNF and ceria particles were 1.3 and 0.1 μm, respectively. In terms of weight, the S20DC to LNF ratio ranged between 10 and 70 wt%. They were screen printed on the $0.89ZrO_2$-$0.10Sc_2O_3$-$0.01Al_2O_3$ electrolyte and sintered at 900°C for 2 h. Then an LNF layer was printed on the sintered active layer and the resulting cell was sintered at 1000 to 1250°C for 2 h in air. The active and LNF current collection layers were approximately 3 and 40 μm thick, respectively.

Cells with an active layer consisting of $Ce_{0.9}Gd_{0.1}O_{1.95}$ (G10DC) and LNF, and $Ce_{0.8}Pr_{0.1}Gd_{0.1}O_{1.9}$ (P10G10DC) and LNF were also prepared. The mean particle size for these doped cerias was about 0.1 μm. A Pt mesh with a pitch of about 100 μm with respect to width and length was attached to the cathode with Pt paste. A Pt anode and a Pt reference electrode were printed on the other side of the electrolyte sheet and the entire peripheral part of the electrolyte sheet, respectively. The effective area of the anode and cathode was 0.785 cm^2 (1.0 cm in diameter). They were finally sintered at 1000°C for 2 h.

2.2. Samples for conductivity measurements

S20DC-LNF composite film samples were also prepared for conductivity measurements. They were screen-printed on Al_2O_3 substrates. Other than their width and length, they were prepared under the same conditions as those used for the S20DC-LNF composite active layer. They were 2 cm long, 5 cm wide and 3 μm thick. The effective length between voltage terminals was about 1 cm. They were sintered at 1000°C for 2 h. Pt paste was used to attach the Pt current and voltage terminals to the films. The samples equipped with the terminals were fired at 900°C for 2 h.

To prepare bulk samples for conductivity measurements, the doped ceria powder was pressed into pellets and sintered in air at 1300°C for 8 h. Then the pellets were cut into rods that were 2 cm long, 0.2 cm wide and 0.2 cm thick. The distance between voltage terminals was about 1 cm.

2.3. Measurements

A single cell was placed in a furnace and humidified H_2 was supplied to the anode. O_2 was supplied to the cathode and reference electrode.[20] The symmetrical geometry of the reference electrode, cathode and anode enabled us to minimize the AC impedance measurement error[21] caused by the misalignment of the cathode and anode,[22] which is estimated to be less than 0.1 mm.

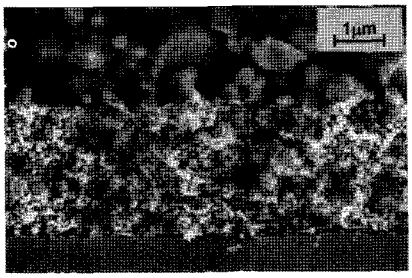

Fig. 1. Back-scattered electron image of typical cross-sections of a cathode.
It is composed of S20DC-LNF composite active layer (50 wt% S20DC) and LNF current collection layer prepared at 1000°C for 2 h.

Before the current was supplied to the cell, the initial value of the interface resistance was measured with an AC impedance analyzer (Solartron SI-1260). The current was controlled so that the signal between the cathode and the reference electrode was less than 5 mV. The AC current frequency was swept from 10^5 to 10^{-1} Hz under open circuit voltage (OCV) conditions. A constant current of 0.2A (0.255 A/cm^2) was supplied between the cathode and anode with a galvanostat at 800°C for about 48 h. Then a high current loading of 1 A/cm^2 was applied for about 4 h. This AC impedance measurement was also conducted after a high current loading. These measurements were conducted 1 h after turning off the constant current.

The DC 4-terminal method was used to measure the conductivity in air of screen-printed films and sintered bulk samples. The temperature of the samples was constantly decreased at 1°C/min and the conductivity was measured.

We used a high-resolution scanning electron microscope (JSM-890 of JEOL) to observe the microstructure of the cathode cross-sections. A back-scattered electron image of the cross-section of the cell near the active layer is shown in Fig. 1.

3. Results and Discussion

3.1. Composition dependence of cathode properties

Fig. 2 shows the temperature dependence of the conductivity of screen-printed S20DC-LNF composite films. When the S20DC is less than 30 wt%, the slope is almost flat. The temperature dependence of the conductivity is similar to that of LNF.[1] This means the LNF particles connect with each other and a long electron path is formed. But in this case, some LNF particles might come into direct contact with the zirconia electrolyte and form $La_2Zr_2O_7$. When the S20DC is 50 wt% or more, the slope is steep and the activation energy is close to that of G10DC (shown in Fig. 8). LNF particles cannot form long chains in those layers, but the S20DC particles can. This can provide an oxide ion conducting path. With this configuration, the LNF particles can contact the zirconia electrolyte via the S20DC particles.

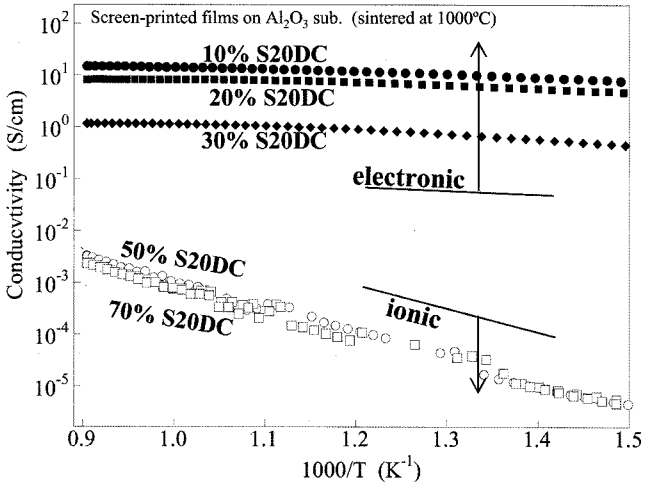

Fig. 2. Temperature dependence of conductivity of screen-printed LNF-S20DC composite films on Al_2O_3 substrates.
They were sintered at 1000°C and measured in air by the DC four terminal method at a cooling rate of 1°C/min. The symbols represent the composition of the films, filled circles for 10 wt% S20DC, filled squares for 20 wt% S20DC, filled diamonds for 30 wt% S20DC, open circles for 50 wt% S20DC and open squares for 70 wt% S20DC.

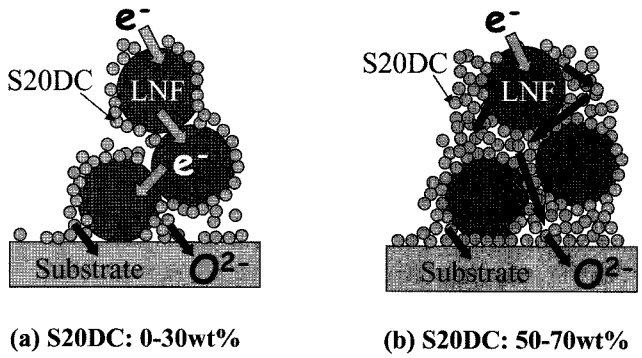

(a) S20DC: 0-30wt% **(b) S20DC: 50-70wt%**

Fig. 3. Schematic diagrams of the microstructure of the LNF-S20DC composite active layer.
(a) S20DC composition is between 0 and 30 wt%. Conduction is electrical. (b) S20DC is 50 wt% or more. The conduction is ionic.

Schematic diagrams of these conduction path geometries are shown in Fig. 3. There appears to be a critical point dividing electronic and ionic conduction at a composition of between 30 and 50 wt% S20DC. Such critical point of conductivity can be explained by the percolation conduction. The known example is the conduction in the Ni-YSZ anode which is composite of the electronic and ionic conductors.[1] When the S20DC is between 30 and 50 wt%, the electronic and ionic paths may block each other. Even in such cases short electronic and ionic conduction paths may be available. Such short paths are sufficient for practical use, because the active layer is two to three times thinner than the LNF particle diameter.

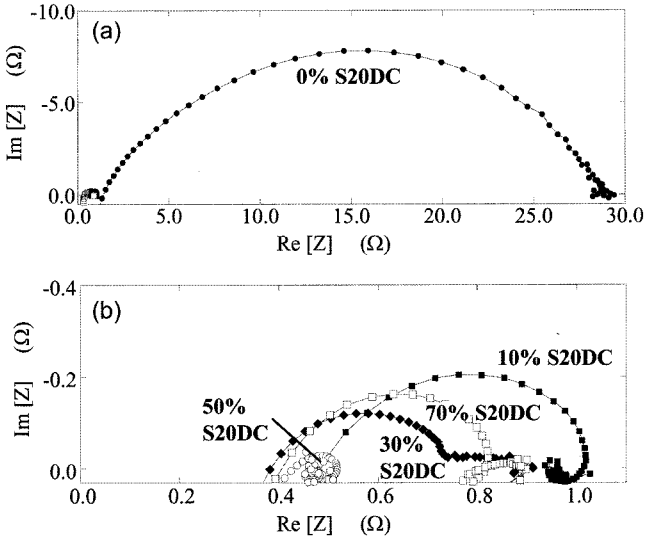

Fig. 4. Composition dependence of the impedance plots of the LNF-S20DC composite cathodes (area: 0.785 cm^2).
They were sintered at 1000°C for 2 h and measured at 800°C before current loading (initial state). Part of Fig. 4(a) is enlarged in Fig. 4(b).

Impedance plots for a cathode with an S20DC-LNF composite active layer are shown in Fig. 4(a) and (b). A portion of Fig. 4(a) is enlarged in Fig. 4(b). These are plots for a cathode with S20DC in the active layer. The measurements were conducted before the current loading. The composition of the active layer ranged from 0 to 70 wt% S20DC. The plot for a 0 wt% S20DC or LNF only cathode has very large interface resistance. This large initial interface resistance stems from $La_2Zr_2O_7$ formation.[13] However, all the composite cathodes had relatively small semi-circles and exhibit good performance. We were concerned that the LNF would contact the electrolyte directly and form $La_2Zr_2O_7$ at the interface when the S20DC was lower than 30wt%. This would degrade the initial cathode performance. But the initial cathode performance was very good including that of a cathode with an active layer containing 10 wt% S20DC. This shows that an active layer containing even a small amount of S20DC can effectively prevent $La_2Zr_2O_7$ formation.

Plots for the cathode after a high current loading of 1 A/cm^2 are shown in Fig. 5. The IR drop or ohmic factor for all the cathodes decreased after the current loading compared with those in Fig. 4. By contrast, the interface resistance tended to increase after the current loading. These changes may be caused by particle grain growth in the composite active layer during the current loading.

In terms of cathode performance, the active layer composition should preferably be around 30~50 wt%. However, when the S20DC is lower than 30 wt%, the adhesion of the active layer (the interface between the composite active layer and $0.89ZrO_2$-$0.10Sc_2O_3$ -$0.01Al_2O_3$ electrolyte) tends to be poor. The adhesion of the 10 wt% S20DC active layer was particularly poor, and the cathode layers were easily

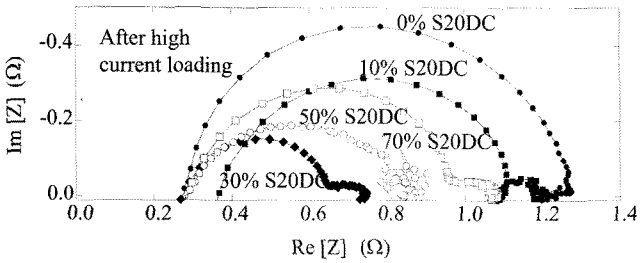

Fig. 5. Composition dependence of the impedance plots of the LNF-S20DC composite cathodes.
They were sintered at 1000°C for 2 h, and measured at 800°C after a high current loading of about 1 A/cm^2.

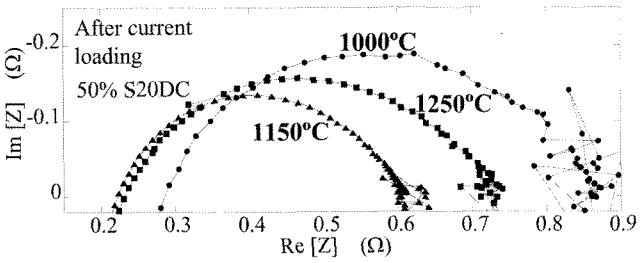

Fig. 7. Sintering temperature dependence of the impedance plots for the LNF-S20DC composite cathodes.
They were sintered at 1000, 1150 and 1250°C for 2 h (50 wt% S20DC, area: 0.785 cm^2). They were measured after a high current loading of about 1 A/cm^2 at 800°C.

scratched away. This appeared to be caused by the configuration of the zirconia and LNF interface, which was connected with very few S20DC particles. Taking interface resistance, adhesion and interface stability into consideration, we selected an S20DC of 50 wt%.

3.2. Sintering temperature dependence

Fig. 6 shows back-scattered electron images of the cross-sections of active layers sintered at different temperatures. The microstructure of the active layer changed with sintering temperature. The S20DC particle size increased at temperatures of 1100°C or above. This was because the S20DC particles are much smaller than those of LNF, thus the temperature dependence of the S20DC sintering is more significant than that for LNF. At a sintering temperature of 1250°C a new layer was formed at the interface between the active layer and $0.89ZrO_2$-$0.10Sc_2O_3$-$0.01Al_2O_3$ zirconia electrolyte. The composition of this layer consists of a solid solution of S20DC and zirconia and LNF.[13,23] Fig. 7 shows impedance plots for a cathode with a 50 wt% S20DC active layer sintered at different temperatures. When the sintering temperature was increased, the ohmic resistance decreased. The interface resistance exhibited its minimum value for a cell sintered at 1150°C. The improvement in the cathode properties with increases in the sintering temperature seems to be caused by a microstructure change.[16] But 1250°C was too high. The interface resistance was larger than that of the cell sintered at 1150°C. This must be related to the newly formed layer at the interface with zirconia.[13,15,23]

3.3. Cathode with cerias doped with different element

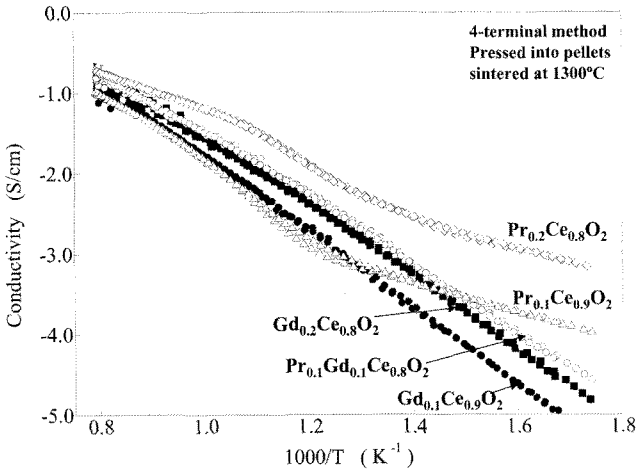

Fig. 8. Temperature dependence of the conductivity of doped ceria bulk samples.
They were pressed and sintered at 1300°C for 8 h, and then measured in air with the DC four terminal method at a cooling rate of 1°C/min. The compositions of the samples were $Gd_{0.1}Ce_{0.9}O_{1.95}$ (filled circles), $Gd_{0.2}Ce_{0.8}O_{1.9}$ (filled squares), $Pr_{0.1}Gd_{0.1}Ce_{0.8}O_{1.95-\delta}$ (open circles), $Pr_{0.2}Ce_{0.8}O_{2-\delta}$ (open diamonds), and $Pr_{0.3}Ce_{0.7}O_{2-\delta}$ (open squares).

We are particularly interested in using Pr-doped cerias for the active layer, because they are mixed conductors.[19] The temperature dependence of the conductivity for pressed and sintered samples doped with ceria is shown in Fig. 8. The temperature dependence (in the lower temperature range) is different from that for Gd doped CeO_2. When the Pr concentration in $Ce_{1-x}Pr_xO_{2-\delta}$ is increased, the total conductivity

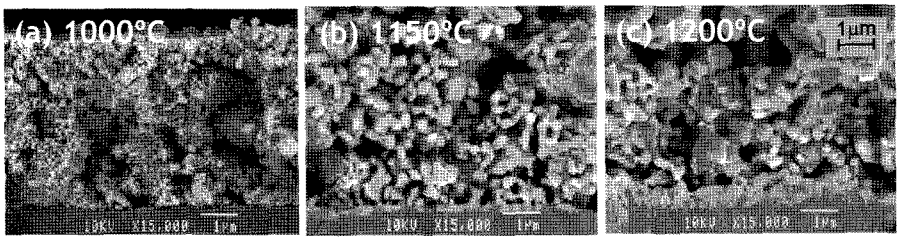

Fig. 6. Back-scattered electron images of S20DC-LNF composite (50 wt% SDC) active layers. They were sintered at (a) 1000°C, (b) 1150°C and (b) 1250°C, for 2 h.

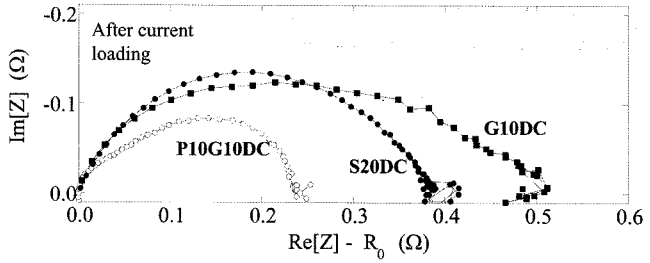

Fig. 9. Impedance spectra for cathodes (50 wt% doped ceria, area: 0.785 cm^2) with active layers whose compositions were S20DC, G10DC and P10G10DC. They were sintered at 1150°C for 2 h and measured at 800°C after a high current loading. The ohmic factor for the cathode was omitted and only interface resistance is shown here.

is increased. When the concentration of Pr was 20 at% (x=0.2), the slope became gentle over the entire temperature range. This suggests that hole conduction exceeded oxide ion conduction for the highly Pr doped CeO_2. With $Ce_{0.8}Pr_{0.1}Gd_{0.1}O_{1.95-\delta}$, the slope was similar to that of $Ce_{0.8}Gd_{0.2}O_{1.9}$, but slightly gentler. This shows that $Ce_{0.8}Pr_{0.1}Gd_{0.1}O_{1.95-\delta}$ is basically an oxide ion conductor. However, $Ce_{0.8}Pr_{0.1}Gd_{0.1}O_{1.95-\delta}$ appeared to be a mixed conductor, and this is obvious from the brown color of $Ce_{0.8}Pr_{0.1}Gd_{0.1}O_{1.95-\delta}$ powder.

Holes, oxygen vacancies and oxygen molecules are available across the entire surface of such mixed conductors. Therefore we expect that the use of Pr-doped ceria for the active layer will increase the TPB. The impedance plots for cathodes with active layers containing ceria doped with Sm, Gd, and Gd and Pr are shown in Fig. 9. They are S20DC, G10DC and P10G10DC. A cathode with an active layer with P10G10DC exhibited the best performance (smaller interface resistance than the others). This may be because the mixed conduction of the Pr-doped ceria expanded the TPB in the active layer. Another different feature of the cathode doped with P10G10DC is that it includes two semi-circles: a very small one around 700 kHz and a large one at 10 Hz. This suggests that two different electrochemical reactions occur during the operation of the cathode with P10G10DC in the active layer.

4. Conclusions

We fabricated single cells with cathodes consisting of an LNF current collection layer and a composite active layer of LNF and doped ceria. We investigated the influence of the composition, the sintering temperature and the dopant in the ceria in the active layer with the AC impedance method. The S20DC-LNF composite active layer was functional when the S20DC was 10~70 wt%, and the cathode exhibited good performance from the beginning. After high current density loading, the ohmic resistance of the cathode decreased. But the interface resistance increased after the loading. In terms of overall performance, the preferred conditions for S20DC active layer preparation are 50 wt% S20DC and sintering at 1150°C. An active layer with P10G10DC has lower interface resistance than those with Gd or Sm-doped ceria. The impedance plots for a cathode with P10G10DC includes two semi-circles: a very small one around 700 kHz and a large one at 10 Hz.

Acknowledgments

We thank Ms. Yoshie Takeuchi for her help with sample preparation. We thank Mr. Masahiro Kato and Mr. Yushi Mita for their help with the cell performance test and conductivity measurements. We also thank Mr. Yoshio Ohki for his help with the SEM observation of our samples.

REFERENCES

1. N. Minh, "Ceramic Fuel Cells," *J. Am. Ceram. Soc.*, **76**, 563-88 (1993).
2. R. Diethelm, M. Schmidt, K. Honegger, and E. Batawi, "Status of the Sulzer Hexis product development," *Proc. 6th Int. Symp. SOFC*, Vol. 99-19, The Electrochemical Society Inc., **199** 60-7 (1999).
3. T. Ishii, "Structural Phase Transition and Ionic Conductivity in $0.88ZrO_2$-$(0.12-x)$ Sc_2O_3-xAl_2O_3," *Solid State Ionics*, **78** 333-38 (1995).
4. H. Orui, K. Nozawa, K. Watanabe, S. Sugita, R. Chiba, T. Komatsu, H. Arai, and M. Arakawa, "Development of Practical Size Anode-Supported Solid Oxide Fuel Cells with Multilayer Anode Structures," *J. Electrochem. Soc.*, **155** B1110-16 (2008).
5. R. Chiba, F. Yoshimura, and Y. Sakurai, "An Investigation of $LaNi_{1-x}$ Fe_xO_3 as a Cathode Material for Solid Oxide Fuel Cells," *Solid State Ionics*, **124** 281-88 (1999).
6. R. Chiba, F. Yoshimura, and Y. Sakurai, "Properties of La_{1-y} $Sr_yNi_{1-x}Fe_xO_3$ as a Cathode Material for a Low-temperature Operating SOFC," *Solid State Ionics*, **152-153**, 575-82 (2002).
7. H. Orui, K. Watanabe, R. Chiba, and M. Arakawa, "Application of $LaNi(Fe)O_3$ as SOFC Cathode," *J. Electrochem. Soc.*, **159** [9] A1412-17 (2004).
8. S. Sugita, H. Arai, Y. Yoshida, H. Orui, and M. Arakawa, "Anode-supported Planar-type SOFC Development at NTT," *J. Electrochem. Soc. Trans.*, **5** [1] 491-96 (2007).
9. H. Orui, K. Nozawa, R. Chiba, T. Komatsu, K. Watanabe, S. Sugita, H. Arai, and M. Arakawa, "Development of Anode Supported Solid Oxide Fuel Cells using $LaNi(Fe)O_3$ for Cathodes," *J. Electrochem. Soc. Trans.*, **7** [1] 255-61 (2007).
10. T. Komatsu, H. Arai, R. Chiba, K. Nozawa, M. Arakawa, and K. Sato, "Cr Poisoning Suppression in Solid Oxide Fuel Cells Using $LaNi(Fe)O_3$ Electrodes," *Electrochem. and Solid-State Lett.*, **9-12** [1] A9 (2006).
11. T. Komatsu, H. Arai, R. Chiba, K. Nozawa, M. Arakawa, and K. Sato, "Long-Term Chemical Stability of $LaNi(Fe)O_3$ as a Cathode Material in Solid Oxide Fuel Cells," *J. Electrochem. Soc.*, **154** B379-82 (2007).
12. T. Komatsu, R. Chiba, H. Arai, and K. Sato, "Chemical Compatibility and Electrochemical Property of Intermedi-

ate-temperature SOFC Cathodes Under Cr Poisoning Condition," *J. Power Sources*, **176** 132-37 (2008).

13. R. Chiba, T. Komatsu, Y. Tabata, H. Orui, K. Nozawa, H. Arai, and M. Arakawa, "Property Change of a $LaNi_{0.6}Fe_{0.4}O_3$ Cathode in the Initial Current Loading Process and the Influence of a Ceria Interlayer," *Solid State Ionics*, **178** 1701-09 (2008).
14. A. Weber, R. Manner, and E. Ivers-Tiffee, "Interaction between Microstructure and Electical Properties of Screen Printed Cathodes in SOFC Single Cells," *Denki Kagaku Oyobi Kogyo Butsuri Kagaku*, **64** 582-89 (1996).
15. E. Ivers-Tiffee, A. Weber, K. Schmid, and V. Krebs, "Macroscale Modeling of Cathode Formation in SOFC," *Solid State Ionics*, **174** 223-32 (2004).
16. R. Chiba, H. Orui, T. Komatsu, Y. Tabata, K. Nozawa, M. Arakawa, K. Sato, and H. Arai, "$LaNi_{0.6}Fe_{0.4}O_3$-Ceria Composite Cathode for SOFCs Operating at Intermediate Temperatures," *J. Electrochem. Soc.*, **155** B575-80 (2008).
17. A. Mai, V. A. Haanapple, S. Uhlenbruck, F. Tietz, and D. Stover, "Ferrite-based Perovskites as Cathode Materials for Anode-supported Solid Oxide Fuel Cells Part I. Variation of Composition," *Solid State Ionics*, **176** 1341-50 (2005).
18. Y. Matsuzaki and I. Yasuda, "Electrochemical Properties of Reduced-temperature SOFCs with Mixed Ionic-electronic Conductors in Electrodes and/or Interlayers," *Solid State Ionics*, **152-153**, 463-68 (2002).
19. S. Lübke and H.-D. Wiemhöfer, "Electronic Conductivity of Gd-doped Ceria with Additional Pr-doping," *Solid State Ionics*, **117** 229-43 (1999).
20. R. Chiba, F. Yoshimura, and Y. Sakurai, "$LaNi_{1-x}Fe_xO_3$ Cathode Material for SOFC Operating at a Reduced Temperature," *Proc. of the Sixth Int. Symp. Solid Oxide Fuel Cells*, Vol. 99-19, The Electrochemical Society Inc., 199, p. 453-62 (1999).
21. Z. Liu, J. S. Wainright, W. Huang, and R. F. Savinell, "Positioning the Reference Electrode in Proton Exchange Membrane Fuel Cells: Calculations of Primary and Secondary Current Distribution," *Electrochimica Acta*, **49** 923-35 (2004).
22. J. Winkler, P. V. Hendriksen, N. Bonanos, and M. Mogensen, "Geometric Requirements of Solid Electrolyte Cells with a Reference Electrode," *J. Electrochem. Soc.*, **155** [4] 1184-92 (1988).
23. H. Arai, R. Chiba, T. Komatsu, H. Orui, S. Sugita, Y. Tabata, K. Nozawa, K. Watanabe, M. Arakawa, and K. Sato, "Reactivity of $LaNi_{0.6}Fe_{0.4}O_3$ with Samaria Doped Ceria," *J. Fuel Cell Technology*, **5** 031204-1- 031204-5 (2008).